Licentiate Thesis:

Physics of Two Dimensional Vortex Glass Models

Petter Holme

Department of Theoretical Physics
Umeå University
November, 2001

Petter Holme
Department of Theoretical Physics
Umeå University
901 87 Umeå, Sweden

E-mail: holme@tp.umu.se
Fax: 090 – 786 9556
Phone: 090 – 786 7760

Abstract

High temperature superconductors have a layered structure and are, due to this low effective dimensionality, believed to be very sensitive to point defects. A possibility exists that the point defects pin the vortices of a penetrating magnetic field into an irregular pattern—a vortex glass. For twelve years models of vortex glass have been studied without any definite conclusions of e.g. their lower critical dimension.

In this Thesis I give an introduction to the vortex glass phase and the studies of phase transitions in disordered systems. I also discuss simulation techniques for zero and finite temperatures. Quantities such as the domain wall energy, the energy barrier for vortex dissipation, the helicity and fourth order moduli, and root-mean square current are all defined and explained.

Many of the discussed topics are applicable to systems of any dimension, but the two papers the Thesis is based on have their scopes restricted to models of two-dimensional superconductors. The results of the papers are presented and put in perspective of other theoretical and experimental works. The main results of the two papers, are that the most studied model, the gauge glass model, has a superconducting low temperature phase; whereas the random pinning model—the most physical model for thin films in magnetic fields—cannot have any finite temperature transition.

Contents

Publications

The Thesis is based on the following papers:

1. Petter Holme and Peter Olsson, *A Zero-Temperature Study of Vortex Mobility in Two-Dimensional Vortex Glass Models*, submitted to Phys. Rev. Lett.

2. Petter Holme, Beom Jun Kim, and Petter Minnhagen, *Phase Transitions in the Two-Dimensional Random Gauge XY Model*, submitted to Phys. Rev. Lett.

Other publications by the Thesis' author:

3. Peter Olsson and Petter Holme, *Comment on "Structure and Phase Transition of Josephson Vortices in Anisotropic High-T_c Superconductors"*, Phys. Rev. Lett. **85**, 2651.

4. Peter Olsson and Petter Holme, *Transition in the two-dimensional step model: A Kosterlitz-Thouless transition in disguise*, Phys. Rev. B **63**, 052407.

5. Beom Jun Kim, H. Hong, Petter Holme, Gun Sang Jeon, Petter Minnhagen, and M. Y. Choi, *XY model in small world networks*, Phys. Rev. E **64**, 056135.

6. Petter Holme and Beom Jun Kim, *Growing scale-free networks with tunable clustering*, accepted for publication in Phys. Rev. E.

Chapter 1

Introduction

The vortex glass phase of high temperature superconductors has been studied for over a decade. Since the idea was first presented, experimentalists have been endowed with numerous new measurement techniques, and theoreticians have already from the start been able to borrow from the well-developed theory of disordered magnetic systems; still, consent on basic aspects of the properties of vortex glass models is lacking to an embarrassing extent.

The main focus of this Thesis is vortex glass models in two dimensions—the limit of thin films or strong anisotropy. In this geometry the possibility of a stable low temperature phase has not been settled. Roughly speaking most studies of most models* of the 2D vortex glass predicts absence of a stable low temperature phase; but there are a few studies that report a critical temperature above zero. In the two papers this Thesis is based on we use some new simulation techniques that, together with a careful consideration of the special aspects of dynamics of disordered systems, I believe, solves this apparent contradiction.

This Thesis is organized as follows: Chapter 2 gives an introduction to the vortex glass phase. Chapter 3 presents the models for the vortex glass. Chapter 4 discusses some concepts of statistical mechanics in general and topics of disordered systems in particular. In Chapters 5 and 6 two very different categories of computational methods for investigating vortex glass models are presented. Finally Chapter 7 summarizes the papers and draws the final conclusions.

*No, not even the question on what model to use is settled.

Chapter 2

The Vortex Glass Phase

The fundamental question motivating this Thesis is whether or not a low temperature superconducting phase can exist in the two-dimensional vortex glass models; so an explanation of the vortex glass phase seems necessary, and that is what Chapter 2 is all about.

2.1 Superconductors in Magnetic Fields

Type-I superconductivity has two major characteristics: zero resistivity and perfect diamagnetism [1, 2], the latter meaning that a magnetic field cannot penetrate the sample while it is superconducting. A type-II superconductor has zero resistivity and perfect diamagnetism at the lowest temperatures; but at higher temperatures magnetic field can penetrate the sample without breaking superconductivity. In this phase the magnetic flux essentially follows "flux tubes" through the material, each carrying one flux quantum $\Phi_0 = h/2e \approx 2.07 \times 10^{-15}\,\mathrm{Tm}^2$. The flux tubes are encirculated by supercurrents, see Fig. 2.1. (I will use the term 'vortex-line' synonymously to flux-tube, and 'vortex' for the intersection between a plane and a vortex-line.)

The flux-tube picture is not entirely true in high temperature superconductors. [3] These have a low density of superconducting electrons and also less confined flux-tubes—but instead regions where magnetic flux and supercurrents can flow simultaneously.

2.2 Effects of Pinning in High Temperature Superconductors

The attachment of a flux tube to the underlying material is called pinning. Pinning is an essential phenomenon for type-II superconductors—without any pinning at all the vortex lattice would start moving when a current is applied, causing dissipation and loss of superconductivity. Pinning can be caused by point defects in the material, or by an anisotropic crystal structure.

A relatively weakly pinned type-II superconductor would have, roughly speaking, the phase diagram shown in Fig. 2.2a. The repulsive interaction between the flux-tubes results in a triangular lattice ("vortex lattice" in Figs. 2.2a and 2.3) which is pinned to the material by point defects, boundary effects, or crystal

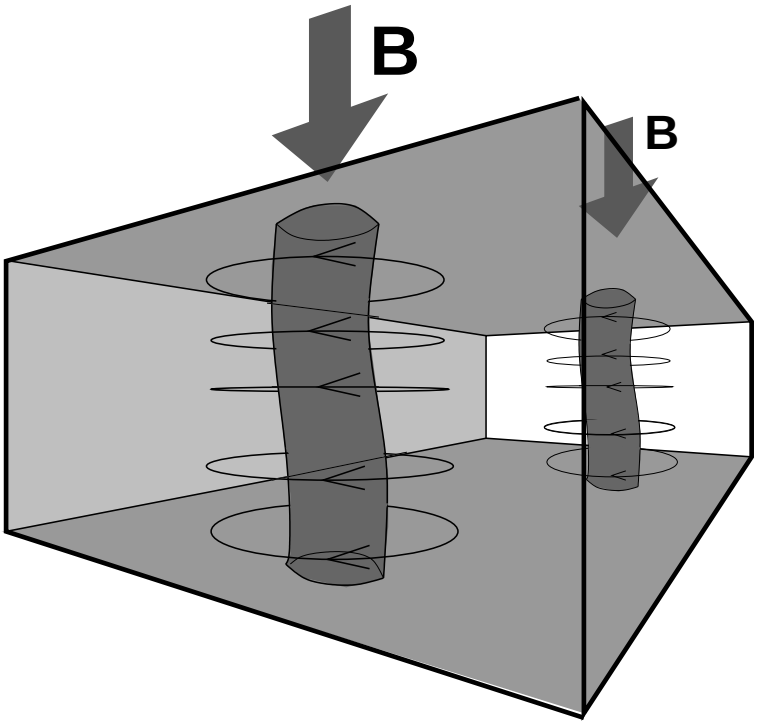

Figure 2.1: *Illustration of magnetic flux penetrating a type-II superconductor through flux tubes, and supercurrent flowing around the flux tubes.*

anisotropy. [4] In the "vortex fluid" phase the flux still penetrates the sample through flux tubes but these are free to move relative to each other, so it is a normally conducting phase.

The high-T_c cuprates are layered materials and in some contexts effectively two dimensional. Point defects will of course affect a two dimensional object much stronger than a three dimensional one. If the interaction between the pinning centers and the vortices become stronger than the vortex-vortex interaction, vortex lines will be pinned in the random fashion that defines the vortex glass phase, see Figs. 2.2b and 2.3. [7] That the random vortex pattern is fixed in time defines long-range glass order. The melting transition of the vortex glass is assumed to take place continuously, as opposed by the first-order melting transition of the vortex lattice. It has been shown analytically that a phase of long-range glass order cannot exist in two dimensions, [5] this does not exclude a low temperature superconducting phase. In fact, models of non-disordered two-dimensional superconductors do not have a low temperature phase with long-range order.

The models of vortex glass that I will present in Chapter 3 are designed to study the vortex-glass to vortex-liquid transitions, other transitions of the phase diagram Fig. 2.2b will not be visible. As the strength of the disorder is easily parametrized, the crossover from the 'pure' picture of Fig. 2.2a to the disordered picture of Fig. 2.2b could also be studied.

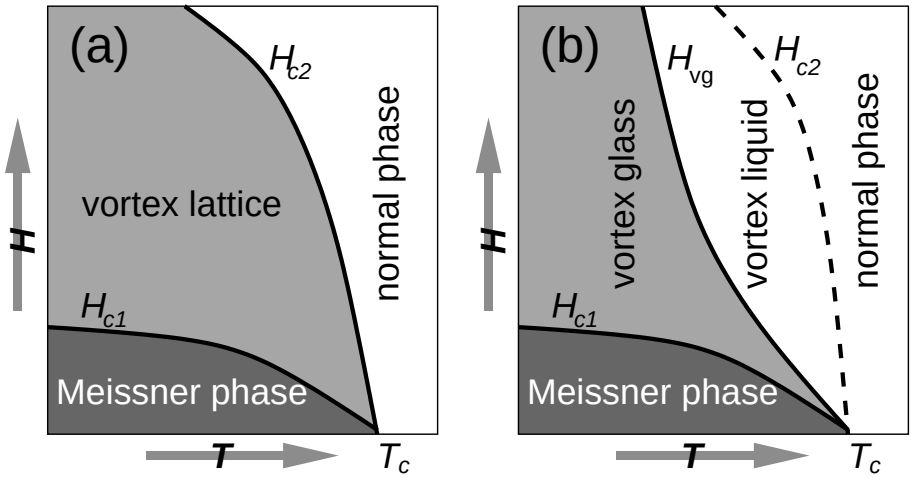

Figure 2.2: ***(a)*** *The standard H-T phase diagram of a conventional type-II superconductor.* ***(b)*** *The proposed phase diagram for high-T_c materials where the vortex-lattice phase is replaced by the superconducting vortex-glass phase and the normal conducting vortex liquid phase. These phase diagrams are dependent on the material and experiment parameters and might have more [6] or less (no vortex glass) phases in some cases.*

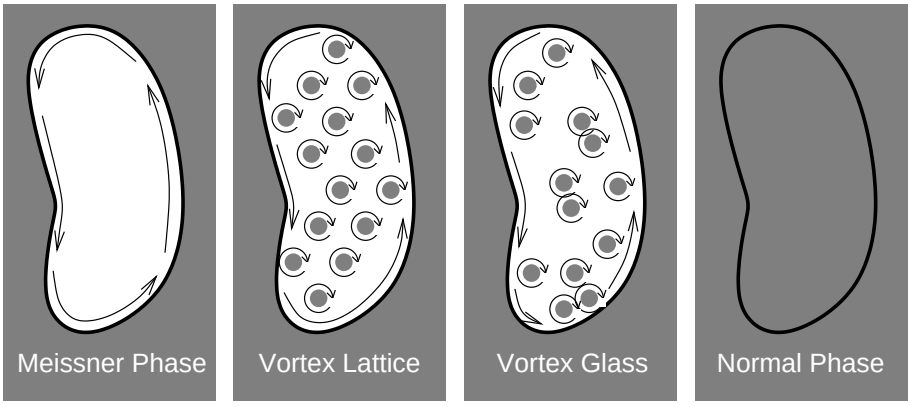

Figure 2.3: *Some phases of a type-II superconductor: The Meissner phase—magnetic field is expelled from the interior. The vortex lattice—vortex lines form a triangular lattice. The vortex glass—vortex lines are randomly pinned by disorder. The normal phase—magnetic flux fully permeates the sample and the supercurrent density is zero. White represents superconducting region and zero magnetic flux density, grey represents normal conducting region. The arrows indicate the supercurrent flow around vortices and the boundary.*

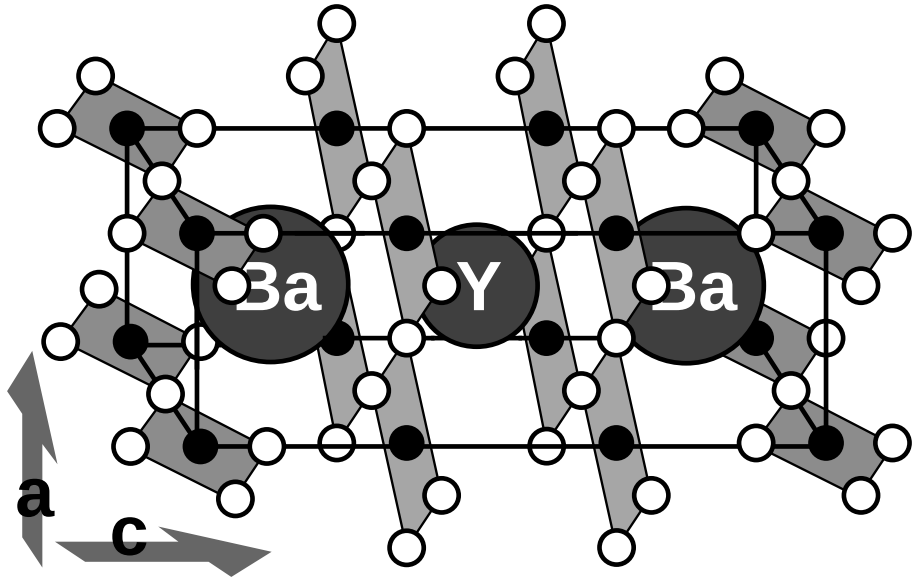

Figure 2.4: *The crystal structure of YBCO. The superconducting planes are normal to the c-axis.* ○ *symbolizes copper atoms, while* ● *symbolizes oxygen atoms.*

2.3 Vortex Glass in Experiments

Much of the experiments on cuprate superconductors have focused on $YBa_2Cu_3O_{7-\delta}$ (YBCO) whose crystal structure is shown in Fig. 2.4. Another commonly used material in experiments is $Bi_2Sr_2CaCu_2O_8$ which is more anisotropic than YBCO, and therefore thought to be even more strongly dominated by two-dimensional effects.

The critical scaling characteristic of the vortex glass transition has been observed in many high-T_c materials. [8] From simulational, and theoretical studies, it is also believed that vortex glass can exist in three dimensions. To eliminate 3D effects in order to test if there is a stable superconducting phase in two dimensions, experimentalists have used thin films. For thinner and thinner films one has observed a loss of a superconductivity [9] which has been taken as a proof that no two-dimensional vortex glass phase exists. But there is at least one other article that reports a finite vortex glass T_c. [10]

Chapter 3

Computational Models for Vortex Glass

All the computational models I will present all have their roots in the phenomenological Ginzburg-Landau theory. [11] The full derivation involves some jumping between levels of description, introducing the relevant features and excluding the irrelevant. I will not go through this here, since it is not necessary for following the rest of the Thesis. For the interested reader I can recommend Ref. [12].

Despite the title of this chapter, I will start by defining two models for investigating phase transitions in clean 2D superconductors. [13] These, the *XY* model and the lattice Coulomb gas model, are the generic models for the study of phase transitions in superconductors, the vortex glass models are in turn motivated from these, rather than derived from a continuum theory.

3.1 The *XY* and Villain Models

The ordinary *XY model* is defined on a discrete lattice by the partition function:

$$Z_{XY} = \prod_i \int_0^{2\pi} \frac{d\theta_i}{2\pi} e^{-\mathcal{H}_{XY}/T} \,, \tag{3.1}$$

where the temperature T (like in the rest of this Thesis) is dimensionless, rescaled by the factor k_B/J, and $\mathcal{H}_{XY}$ is the Hamiltonian:

$$\mathcal{H}_{XY} = -\sum_{(i,j)_{\mathrm{nn}}} \cos(\phi_{ij} \equiv \theta_i - \theta_j) \,, \tag{3.2}$$

and $\theta_i \in [-\pi, \pi)$ is a variable associated with lattice point i, and the sum is over nearest neighbor pairs $(i,j)_{\mathrm{nn}}$. Quantities of dimension energy, such as $\mathcal{H}_{XY}$, are made dimensionless by scaling a factor $1/J$, where J is known as the *Josephson coupling strength*.

The *XY* model is a general model for studies of superconductors, superconducting arrays, and superfluids, and at least its static properties are by now quite fully understood. The physics of the *XY* model is governed by vortex (or, in 3D, vortex line) interaction—a vortex in the *XY* model is a point with non-zero rotation, corresponding to the flux tubes in the real world discussed

in Section 2.1:*

$$q(\mathbf{r}) = \sum_{\square_{\mathbf{r}}} \|\phi_{ij}\|_{[-\pi,\pi)} \ , \tag{3.3}$$

where the sums are to be taken over the plaquette at $\mathbf{r}$, and $\| \cdots \|_{[-\pi,\pi)}$ is to be read "in the interval $[-\pi, \pi)$".

In the *Villain model* [14] the cosine interaction potential of the XY model is replaced by U defined through:

$$e^{-U(\phi)/T} = \sum_{n=-\infty}^{\infty} e^{-(\phi-2\pi n)^2/2T} \ . \tag{3.4}$$

3.2 The Lattice Coulomb Gas Model

As mentioned above, the vortices are believed to qualitatively determine the physics of the spin models of Sect. 3.1; whereas the other excitations, the *spin waves*, merely change the value of the transition temperatures. The energy for separating a vortex pair a distance r is known to be proportional to $\log r$; this is in analogy with the *2D lattice Coulomb gas*, defined by the grand partition function:

$$\mathcal{Z}_{\mathrm{CG}} = \sum_{N=0}^{\infty} \left[\frac{N}{2}!\right]^{-2} \int_{-\infty}^{\infty} \prod_{i=1}^{N} \frac{d\mathbf{r}_i}{\zeta} e^{-\mathcal{H}_{\mathrm{CG}}/T} \ , \tag{3.5}$$

where $\zeta \sim r_0^2$ is the *phase space division*, r_0 is the charge's linear dimension and $\mathcal{H}_{\mathrm{CG}}$ is the Hamiltonian for an N-particle configuration:

$$\mathcal{H}_{\mathrm{CG}} = -\frac{1}{2} \sum_{i \neq j} Q_i \, Q_j \ln r_{ij} + N \, T^{\mathrm{CG}} \ln z \ , \tag{3.6}$$

where $Q_i \in \{-1, 1\}$ is the charge of particle i. z is known as the *fugacity* (and can be interpreted through $-2\,T^{\mathrm{CG}} \ln z$ being the energy for creating a dipole of separation r_0).

For computational reasons one often sums over the discretized space rather than the Coulomb gas (CG) particles. The effective phase variables then changes from $\{Q_i\}$ to the charge per lattice point $\{q_i\}$, and the ensemble changes from the grand canonical to the canonical. The Hamiltonian then becomes:

$$\mathcal{H}_{\mathrm{CG}} = -\frac{1}{2} \sum_{\mathbf{r} \neq \mathbf{r}'} q_{\mathbf{r}} \, q_{\mathbf{r}'} \, G(\mathbf{r} - \mathbf{r}') \ , \tag{3.7}$$

where G is the lattice Green's function, in the 2D square lattice case:

$$G(\mathbf{r}) = \left(\frac{2\pi}{L}\right)^2 \sum_{\mathbf{k} \neq 0} \frac{\exp(i\mathbf{k} \cdot \mathbf{r}) - 1}{4 - 2\cos k_x - 2\cos k_y} \ . \tag{3.8}$$

*In the literature one often sees the same terms signifying elements from both the simulation model, continuum theory, and real world superconductors. This is the case for 'vortex', and most of the model parameters. The reader should be cautious.

The advantage of the Villain interaction potential (see Sect. 3.1), is that it makes vortex and spin wave excitations separable. Thus there exists a exact (surjective) mapping from the spin- to the CG-representation. [15]

The 2D CG model has been shown to have qualitatively the same phase diagram as the 2D XY model, which *a posteriori* justifies the reduction of the model.

The zero temperature methods that will be discussed in Chapter 5 are all based on the CG picture (since no spin waves exists at $T = 0$). The mapping from spin to CG picture is defined by Eq. (3.3).

3.3 The Random Gauge XY Model

The *random gauge XY model* is a modification of the standard XY model, made to study the vortex glass to vortex liquid transition.[†] In this model the disorder enters the problem as a quenched (time invariant) random vector potential. The Hamiltonian is:

$$\mathcal{H}_{\mathrm{RG}XY} = \sum_{(i,j)_{\mathrm{nn}}} U\left(\phi_{ij} \equiv \theta_i - \theta_j - A_{ij}\right) \ , \tag{3.9}$$

where the A_{ij}s are random variables of a rectangular distribution in the interval $[-r\pi, r\pi]$. r is called the *disorder strength* and is restricted to the interval $[0, 1]$. $r = 0$ gives the ordinary XY model, and in the maximally disordered limit $r = 1$ the model is called the *gauge glass model*.

The interaction potential U is often taken to be the $-\cos$ of the XY model, but can also be chosen to be the Villain potential. In zero temperature studies the Villain potential is more natural, while for the Monte Carlo simulations one uses the cosine potential (by tradition). This change of interaction potential is not expected to result in any qualitative difference.

In the CG picture (obtained through Eq. (3.3)) the vortex charges of the random gauge XY model belongs to $\{\varphi_i + n : n \in \mathbb{Z}\}$ where $\varphi_i \in [-1, 1)$ is determined by:

$$\varphi_i = \frac{1}{2\pi} \sum_{\square_{\mathrm{r}}} \| - A_{ij}\|_{[-\pi,\pi)} \ . \tag{3.10}$$

3.4 The XY Spin Glass Model

In the *XY spin glass model* a randomly selected set of links are antiperiodic. The Hamiltonian is given by:

$$\mathcal{H}_{\mathrm{XYSG}} = \sum_{(i,j)_{\mathrm{nn}}} j_{ij}\, U\left(\phi_{ij} \equiv \theta_i - \theta_j\right) \ \text{ where } \ j_{ij} \in \{-1, 1\} \ . \tag{3.11}$$

Disorder strength is parametrized by s—the probability for $j_{ij} = -1$.

The vortex charges of the XY spin glass model (see Eq. (3.3)) belongs to

$$\{\varphi_i + n : n \in \mathbb{Z}\} \ \text{ where } \ \varphi_i \in \{0, 1/2\} \ . \tag{3.12}$$

[†]To be exact, it is designed to study any superconducting to normal conducting transition in a disordered material.

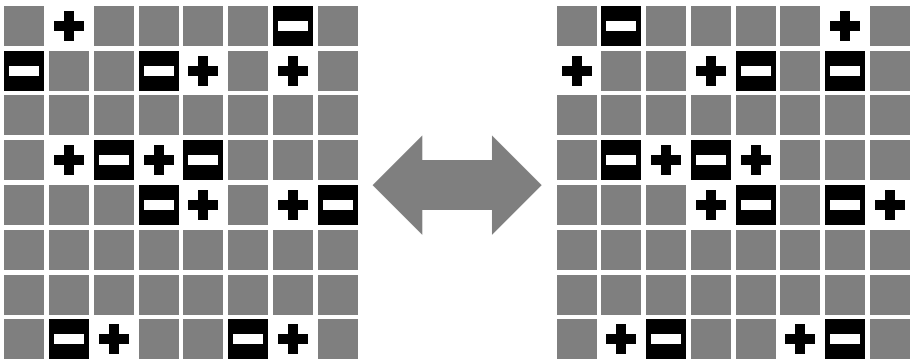

Figure 3.1: *Two chirally opposite ground states of a realization of a* 8×8 *XY spin-glass system with disorder density* $s = 0.15$. ▩ *represents zero charge,* ✚ *means a* $+1/2$ *charge and* ▬ *means a* $-1/2$ *charge.*

Hence there is a possibility for *chiral order*, where reflective symmetry is spontaneously broken, in the *XY* spin glass. The phase space could be divided into two disconnected sets distinguished by opposite local chiralities $\kappa(\mathbf{r})$:

$$\kappa(\mathbf{r}) \equiv \sum_{\square_\mathbf{r}} U'(\phi_{ij}) \; . \tag{3.13}$$

With harmonic potential (a Villain potential at $T = 0$) $\kappa(\mathbf{r})$ just reduces to the Coulomb charge $q_\mathbf{r}$.

$$\kappa(\mathbf{r}) = \sum_{\square_\mathbf{r}} U'(\phi_{ij}) = \sum_{\square_\mathbf{r}} \| \phi_{ij} \|_{[-\pi,\pi)} = q_\mathbf{r} \; , \tag{3.14}$$

where notations are those of Eq. (3.3). If $\Theta = \{\theta_i\}$ is a ground state spin configuration then so is its chirally inverted image $\widetilde{\Theta} = \{\widetilde{\theta}_i \equiv 2\theta' - \theta_i\}$, where θ' is the *mirror angle*. Let $Q = \{q_i\}$ be the Coulomb gas configuration corresponding to Θ, then $\widetilde{Q} = \{\widetilde{q}_i \equiv -q_i\}$ is the Coulomb gas configuration corresponding to $\widetilde{\Theta}$, see Fig. 3.1. This also shows that in contrast to the random gauge *XY* model the ground state of the *XY* spin glass model is always degenerate, for every L.

3.5 The Random Pinning Model

The apparently most unphysical feature of the random gauge *XY* model and the *XY* spin glass model is that the average frustration (magnetic field) is zero.[‡] In remedy one can define the following lattice Coulomb gas type of model, the *random pinning model*: [16]

$$\mathcal{H}_{\mathrm{rp}} = -\frac{1}{2} \sum_{\mathbf{r} \neq \mathbf{r}'} (q_\mathbf{r} - f) \, G(\mathbf{r} - \mathbf{r}') \, (q_{\mathbf{r}'} - f) - \sum_\mathbf{r} v_\mathbf{r} \, q_\mathbf{r}^2 \; . \tag{3.15}$$

[‡]Of course, the random gauge *XY* model and the *XY* spin glass model can be very physical models of other disordered systems.

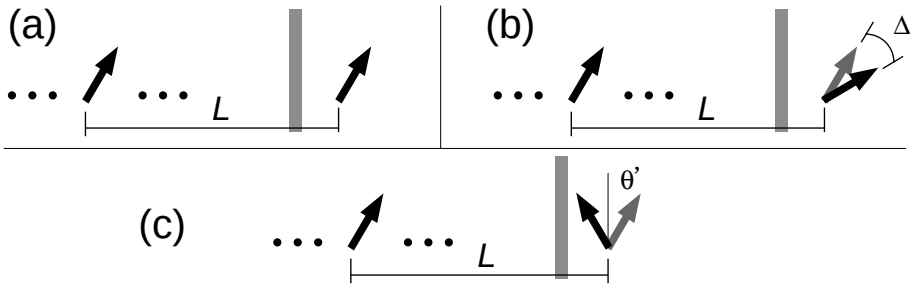

Figure 3.2: *Different boundary conditions.* ***(a)*** *Periodic boundary condition: If a spin looks across the boundary a distance L (the linear dimension of the system) it will see itself.* ***(b)*** *Twist boundary condition: If a spin looks across the boundary a distance L it will see itself rotated an angle* Δ. ***(c)*** *Reflective boundary condition: If a spin looks across the boundary a distance L it will see itself mirrored in an angle* θ'.

The frustration here is homogeneous and the disorder enters the Hamiltonian through the pinning potential $v_{\mathbf{r}}$, which is chosen to have a rectangular distribution in the interval $[-\pi, \pi]$. To avoid that positive ($v_{\mathbf{r}} > 0$) pinning centers can get arbitrary high vorticity we restrict the possible values of $q_{\mathbf{r}}$ to $\{-1, 0, 1\}$.

3.6 Other Models

In the three models above, the vortex interaction is unscreened which is believed to be physical in the low-vortex limit (i.e. for the lowest temperatures). Some studies have been based on models including the screening. I will not present the models here, since the results (as expected) are qualitatively the same as for unscreened models. The interested are recommended the articles of Ref. [17].

3.7 Boundary Conditions

In many branches of physics, the question of what boundary condition to use is solved by looking at the physical situation: If a liquid is free to flow in and out of a system, an open boundary condition is used, and so on. In computational statistical mechanics the boundary condition is often a tool for study order and symmetries the system. For example, one can detect chiral order by the reflective boundary condition, or study magnetic transitions through the antiperiodic boundary condition. Three basic boundary conditions of this Thesis are defined in Fig. 3.2.

The twist boundary condition (see Fig. 3.2b) is useful for studying the XY model. One essential application is to add the twist angles to the degrees of freedom through the extra term $-\mathbf{r} \cdot \Delta / L$ in the argument of the Hamiltonian's interaction potential ($\mathbf{r} = (r_x, r_y)$ is the coordinates of θ_i). (See Eqs. (3.9) and (3.11).) The model with the new boundary condition and degrees of freedom is said to have *fluctuating twist boundary condition* (FTBC) [18]. This has many practical advantages: E.g. vortex lattices of the ordinary XY model are more

easily formed. In vortex glass models finite system size makes the net current of the ground state non-zero, this makes some quantities harder to converge, this can be solved by finding a twist that zeroes the current by using FTBC. FTBC also has the important quality to be the equivalent of periodic boundary condition for vortex interaction; and as long as the effect of a new boundary condition disappears in the thermodynamic limit it is safe to use.

Chapter 4

Some Concepts of Statistical Mechanics

This chapter aims to introduce some basic concepts of the study of phase transitions that is used in the rest of the Thesis. To save the print cost of an additional 500 pages I did not make this chapter a general introduction to the subject, the interested reader is recommended Ref. [19] for a general introduction, or Ref. [20] for an introduction to the theory of phase transitions in disordered systems. The first three sections of this chapter focus on the change of symmetry at a phase transition. The last section discusses how one can use finite size effects to get true critical parameter values.

Central for the first three sections is the *phase space* or *configuration space* Σ—the space whose coordinates are the degrees of freedom of the system:

$$\Sigma = \bigotimes_i \mathcal{P}_i \,, \tag{4.1}$$

where $\{p_i : p_i \in \mathcal{P}_i\}$ is the degrees of freedom, $\mathcal{P}_i$ is the possible values for the i'th degree of freedom, and $\otimes$ denotes the Cartesian product. In the spin models of Sects. 3.1, 3.3, and 3.4 the degrees of freedom are the spin and twist variables that are defined over the interval $[-\pi, \pi)$. In the CG picture the degrees of freedom are the vorticity charges with $\mathcal{P}_i = \{\varphi_i + n : n \in \mathbb{Z}\}$, where φ_i is determined by disorder (see Eqs. (3.10), (3.12), and (3.15)).

4.1 Ergodicity Breaking

We start with an example—the 2D Ising model on an $L \times L$ square lattice. The Ising model is a spin model quite similar to the XY model, what differs is that the spin degrees of freedom s_i only take discrete values $s_i \in \{-1, 1\}$. The Hamiltonian is:

$$\mathcal{H}_{\text{Ising}} = -\sum_{(i,j)_{\text{nn}}} s_i s_j \,. \tag{4.2}$$

Order in the Ising model can be described by the *magnetization*

$$M = \frac{1}{L^2} \sum_i s_i \,. \tag{4.3}$$

In the thermodynamic limit ($L \to \infty$) there is a critical temperature $T_c = 2/\sinh^{-1} 1 \approx 2.27$. Above this temperature both time and ensemble av-

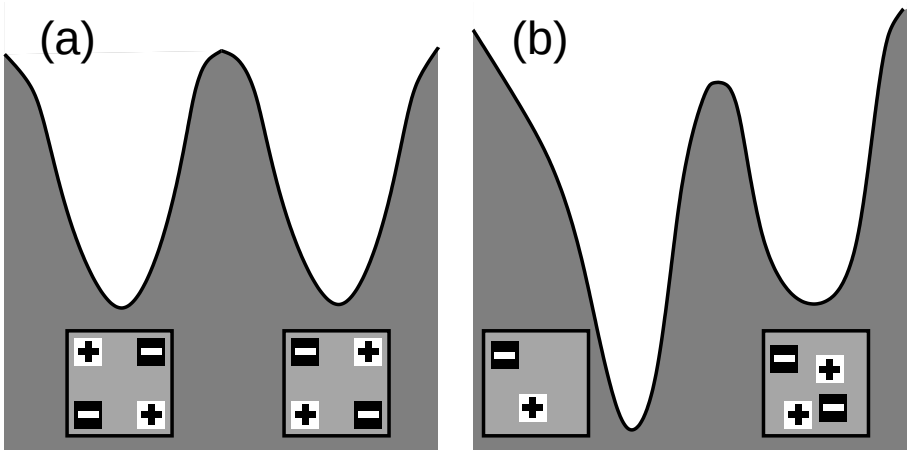

Figure 4.1: *Spontaneous symmetry breaking (a) and replica symmetry breaking (b). The profile represents the energy versus phase space coordinate (the phase space is represented by the one-dimensional horizontal axis). Imagine the energy barrier growing to infinity at T_c, then the system is trapped in one of the two regions of phase space. In (a) these regions are related by symmetry, in (b) the minima are asymmetric. The square containing the ✚ and ▬ gives a more detailed illustration of the configurations corresponding to the two minima. The figures resemblance to other figures used to discuss vortex glass models is almost accidental—this is just an illustration*

erages of M are zero. That is, a dynamical simulation of the system would produce the same average M as a direct summation according to the Boltzmann distribution would do. Below T_c a time average of M is non-zero, whereas a ensemble average is still $M = 0$. When, at a phase transition, time and ensemble average starts to differ *ergodicity breaking* has occurred. If ergodicity is broken, the phase space is effectively partitioned into mutually unreachable subsets. When restricted to these subsets (or *restricted ensembles*) Boltzmann statistics is assumed to apply. In the case of the 2D Ising model the phase space is partitioned into one subset with positive and one subset with negative magnetization. These two disjoint subsets are related by reflection $s_i \mapsto -s_i$: If $\{s_i\}$ belongs to the subset with positive magnetization, then $\{-s_i\}$ belongs to the subset with negative magnetization. An ergodicity breaking where the isolated subsets are related by symmetry (such as reflection), is called *spontaneous symmetry breaking*.

4.2 Replica Symmetry Breaking

For some systems there are different ways for the system to order that are not related by symmetry, if this is the case one says that the *replica symmetry* is broken. [21] In Figure 4.1 the spontaneous symmetry breaking is compared to replica symmetry breaking. Two principal complications arises when replica symmetry breaking occurs: 1. It is usually very hard to specify an isolated subset of the phase space, and therefore to calculate the expectation values of physical quantities in that region. 2. Non-symmetry-related isolated subsets might

yield different values of certain quantities, since they correspond to ordering of different symmetry.

One model where replica symmetry breaking is believed to occur [22] is the 3D Ising spin glass defined by the Hamiltonian:

$$\mathcal{H} = \sum_{(i,j)_{\rm nn}} j_{ij} s_i s_j \,, \tag{4.4}$$

where $j_{ij} \in \{-1, 1\}$ are randomly distributed quenched variables.

The magnetization in the Ising model and the Ising spin glass is a *local order parameter*: Order parameter in the sense that if it's time average is zero then the system has no order (and vice versa); local in the sense that it can be averaged over an arbitrarily small region in phase space to monitor the order of that particular region. For studying the magnetization when replica symmetry is broken one can calculate the *replica overlap* of the magnetization:

$$q(\sigma, \sigma') = \lim_{L\to\infty} \frac{1}{L^2} \sum_i m_i^\sigma \, m_i^{\sigma'} \,, \tag{4.5}$$

where σ and σ' are two ergodic regions of the phase space, and m_i^σ and $m_i^{\sigma'}$ are the ensemble average of the spin s_i with the ensemble restricted to the respective region. If replica symmetry is unbroken, the probability distribution of q, $[P(q)]$, (for all choices of σ and σ', and all possible realizations of the disorder) is non-zero at exactly one value of q; if replica symmetry is broken more than one (possibly infinitely many) values q have non-zero expectation values. One of the great advantages of $[P(q)]$ is that it by definition is obtained by summing over the whole phase space. This means that one does not have to simulate the system with the slow physical dynamics, but instead can concentrate on sampling the phase space without bias (a purpose for which well-developed methods exists).

For the XY type models in two dimensions there is no local order parameter such as the magnetization in the Ising model and the Ising spin glass. This means that there is no way of defining an overlap function of the form Eq. (4.5) that can serve both as an order parameter and an indicator of replica symmetry breaking (in the way $[P(q)]$ did above). Instead one has to use other, more indirect, methods to detect order and replica symmetry breaking (that will be discussed in Sects. 5.1 and 6.5).

4.3 Critical Finite Size Scaling

The size-dependence of certain quantities close to a critical temperature often follows simple power-law relations. This can be exploit to determine the critical values of environment variables, such as temperature. I will only sketch underlying the idea and state the practical method, not give a thorough analytical discussion. The analytically minded reader is referred to Refs. [19, 23].

Let A be a quantity that close to the transition temperature follows the power-law relation $A \sim |T - T_c|^a$, $a > 0$. Then the standard finite size scaling of A close to T_c is based on the assumptions that:

1. A does not depend separately on correlation length* ξ and L close to the transition, but on ξ/L.

2. ξ/L diverges as
$$\xi/L \sim |T - T_c|^{-\nu} \ , \ \nu > 0 \ , \tag{4.6}$$
close to the transition.

This means that close to the transition we can write:

$$A_L = |T - T_c|^a \, F(\xi/L) \ , \tag{4.7}$$

A_L being the expectation value of A for a system of linear dimension L, and F a smooth function. Combining Eqs. (4.6) and (4.7) gives:

$$A_L = \left(\frac{\xi}{L}\right)^{-a/\nu} F\left(\frac{|T - T_c|^{-\nu}}{L}\right) = L^{-b} f\left(L^{1/\nu}(T - T_c)\right) \ , \tag{4.8}$$

where $b = a/\nu$ and f a smooth function.

From Eq. (4.8) one can deduce a procedure for determining T_c and the exponents b and ν from the temperature and size dependence of A: First, at T_c, $A_L L^b$ is constant with respect to L. Thus curves of different L of a plot of $A_L L^b$ versus temperature should all cross at T_c for the correct exponent b. Second, when T_c and b is known, all $A_L L^b$-curves should collapse into one as a function of $L^{1/\nu}(T - T_c)$ for the correct value of ν in a neighborhood of T_c.

Now everything is not always that simple—fluctuations in environment parameters (such as temperature) might result in corrections to this scaling form, but in this Thesis such corrections will not be considered.

4.4 Notations for Averages

To avoid confusion I will use the following notations for the different types of averages:

$\langle \cdots \rangle$	Unspecified average.
$\langle \cdots \rangle_t$	Time average (of a simulation with some specific dynamics).
$\langle \cdots \rangle_{\mathrm{e}}$	Ensemble average (average over the whole configuration space according to Boltzmann statistics).
$\langle \cdots \rangle_{\mathrm{re}}$	Average over a restricted ensemble (see Sect. 4.1) if ergodicity is broken, otherwise identical to $\langle \cdots \rangle_{\mathrm{e}}$.
$[\cdots]$	Average over disorder realizations.

*The correlation length is the length scale over which correlations decay. Roughly speaking, it is the linear size of the area around a point where the system looks the same. A precise definition can be found in Ref. [19].

4.5 Self-Averaging

Suppose that we, in a finite-size system of dimension L, make n independent measurements of a quantity A_L. Consider the error ΔA of the thermodynamic quantity $A = \lim_{L\to\infty} A_L$:

$$\Delta A(L,n) = \sqrt{\frac{\langle A_L^2\rangle_{\rm e} - \langle A_L\rangle_{\rm e}^2}{n}} \; . \tag{4.9}$$

If $\lim_{L\to\infty} \Delta A(L,n) = 0$ for any sufficiently large n, the system is said to be *self-averaging* with respect to A.

If the averages of Eq. (4.9) are over realizations of disorder,

$$\Delta A(L,n) = \sqrt{\frac{[A_L^2] - [A_L]^2}{n}} \; , \tag{4.10}$$

and the quantity A_L is known to infinite precision for every disorder realization, then if $\lim_{L\to\infty} \Delta A(L,n) = 0$ the system is said to be *disorder self-averaging* with respect to A. Disorder self-averaging is often implicitly assumed in disordered systems. But when replica symmetry is broken it is not trivial that all quantities are disorder self-averaging, so I will discuss the system's disorder self-averaging of important quantities after they are introduced.

Chapter 5

Zero Temperature Methods

In models without disorder the ground state itself is seldom very informative. However, disordered models like the ones discussed in Sections 3.3, 3.4 and 3.5, have a non-trivial ground state; a fact that can be used to draw conclusions for finite temperatures properties. In generalizing zero temperature results to finite temperatures there are many subtleties, for example, for the XY spin glass model, the ground state is degenerate in the thermodynamic limit, which cannot be the case in real systems.

The basic idea of zero temperature studies is to see how the energies for different types of energy barriers in the system scales with the system size L. If a certain low-temperature phase needs a specific energy barrier to retain order, and this energy barrier is finite for $L \to \infty$, then the system cannot have that low-T phase , since there would be a finite probability for that barrier to be surpassed at any finite temperature.

This Chapter starts with a discussion on the consequences of a replica symmetry breaking, then discusses two types of energy barriers, and finishes with three sections on computation techniques.

5.1 Replica Symmetry Breaking and Dynamical Assumptions

When ergodicity breaking can occur, not only the values of dynamical but also static quantities can be affected by the explicit dynamics of a system, since different dynamics might break the phase space in different ways. As an example we can consider the *helicity modulus*:

In non-disordered superconductors the helicity modulus Υ is directly related to the superconductivity properties of the material: If $\Upsilon > 0$ the substance is superconducting, if $\Upsilon = 0$ it's not. For disordered systems this is also believed to be true, although a proper renormalization group treatment is (to my knowledge) lacking. By definition Υ is the second order derivative of the free energy with respect to twist:

$$\Upsilon = \left. \frac{\partial^2 F}{\partial \Delta^2} \right|_{\Delta=\Delta_0} , \tag{5.1}$$

where Δ_0 gives the global minimum of the free energy, and the free energy is defined as an ensemble average.

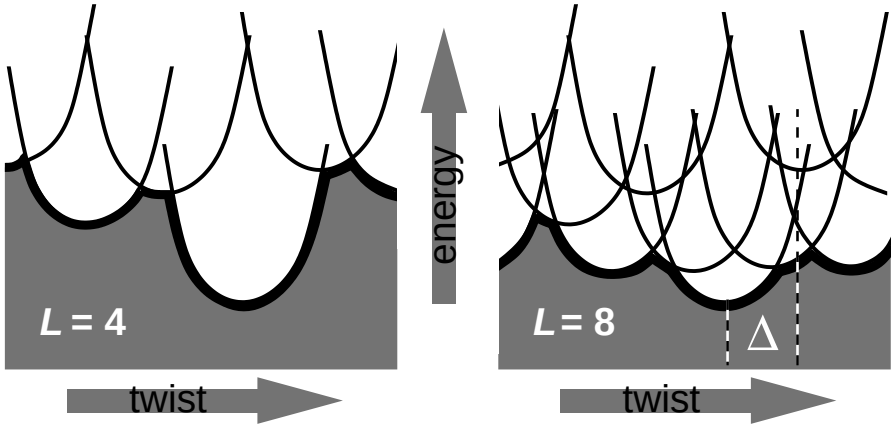

Figure 5.1: *The free-energy versus twist landscape for increasing L. If one looks a short distance Δ to the right the energy landscape looks completely different if the dynamics allow vortex tunneling (thick lines) or not (thin parables). This figure shows only the least energetic parable centered at position* $\Delta_0 + 2n\pi/L$.

The question is now the time average, which is the average that will be measured in real experiments. To be specific, let's consider the gauge glass model with Villain potential (see Section 3.3). In this case the free-energy versus twist landscape will consist of parables:

$$F_i(\Delta) = \frac{1}{2}\left(\Delta - \Delta_0 - n\frac{2\pi}{L}\right)^2 + \epsilon_i \ , \tag{5.2}$$

where $n = n(i) \in \{0, \cdots, L-1\}$, i is the index of the CG configuration corresponding to the parable,* and ϵ_i is a function of the disorder. As $L \to \infty$ the more and more parables will "eat up" the energy landscape so it becomes totally flat.† (See Fig. 5.1.) Let Υ_{e} represent the helicity modulus when the free energy is defined as a ensemble average, and let Υ_{re} denote the helicity modulus for a free energy averaged over a restricted ensemble A flat landscape have $\Upsilon = \Upsilon_{\mathrm{e}} = 0$ as long as Boltzmann statistics is applicable. But if ergodicity is broken in such a way that the parables neighboring a ground state not is accessible,‡ the physically relevant ensemble has a F with finite curvature at every point, even in the thermodynamic limit, so the helicity modulus is $\Upsilon = \Upsilon_{\mathrm{re}} = 1$.

Despite its title I have used the phrase "ergodicity breaking" throughout this section. The asymmetric frustration of the vortex glass models makes er-

* There is an enumerable infinite number of CG configurations, most of these are one dipole excitation away from a configuration with lower energy, and hence not a local minimum. There are on the other hand nothing that prevents several local minima with the same polarization. I.e., there might be many i with the same n.

ϵ_i is the energy of different CG configurations. The parables corresponds to the energy increase from a net current over the system. For the standard XY model with a Villain potential, the whole free-energy versus twist space is one parable centered around $\Delta = 0$.

† This is best measured by the domain wall energy, discussed later (in Section 5.4).

‡ This is a conclusion we will be able to draw later from the scaling of Υ and V_L—see Sect. 5.2, and Paper 1.

godicity breaking to automatically imply replica symmetry breaking. But since all parables looks the same, the discussion about the helicity modulus is independent of the type of ergodicity breaking. If one instead considers the energy of the system, things are different. If every parable represents an isolated part of the phase space (in the low temperature phase) then the value of the energy will differ for different realizations of an experiment, and the system would not be disorder self-averaging for energy, but it would be for the helicity modulus. But, as mentioned, it is very hard to determine the isolated regions of the phase space—much harder than to see whether ergodicity is broken or not.

In all the vortex glass models in the Sections 3.3, 3.4 and 3.5, the possibility of replica symmetry breaking is dependent on the vortex dynamics: whether one allows quantum tunneling of vortices, or if vorticity is locally conserved. There are theories and experimental evidence for quantum tunneling of vortices [24], but these are seldom brought into the framework of standard models of superconductors. With quantum tunneling of vortices the vortex glass models would retain replica symmetry at all temperatures, but with local vorticity conservation this is far from trivial.

5.2 The Energy Barrier for Vortex Dissipation

That vorticity transport over arbitrary distances is prohibited is a prerequisite for a superconducting phase. In dynamical simulations [26] the relaxation time τ is taken to be the average the time for a vorticity transport of one unity charge across the system; and resistivity is inversely proportional to τ. In the phase representation of the XY model this corresponds to a 2π change of the global twist Δ, and is thus termed a "2π phase slip".

A more technical definition of the energy barrier for vortex dissipation (or a 2π phase slip) V_L, would be: Starting from the ground state, let $\mathcal{P}$ be a path that regenerates the ground state and has a net polarization change of L (which equals a twist change of 2π in the spin picture). (A path being a sequence of vortex dipole excitations.) Then, let $\widetilde{V}_L(\mathcal{P})$ denote the energy, relative to the ground state, of the most energetic configuration of $\mathcal{P}$. The barrier energy for the configuration in question $\widetilde{V}_L$ is then simply the minimum of $\widetilde{V}_L(\mathcal{P})$ for all $\mathcal{P}$. Finally let V_L be $\widetilde{V}_L$ averaged over disorder realizations. A path for an actual realization of a 4×4 gauge glass system, giving the minimum energy barrier $\widetilde{V}_L$ is shown in Fig. 5.2.

5.3 The Energy Barrier for Chiral Mirroring

To investigate the possibility of chiral order in the XY spin glass model, one can measure the energy barrier between the subsets of opposite chirality (see Section 3.4). To do that one has to modify the definition of V_L a little: For every ground state $\{q_i\}$ (remember that the ground state is degenerate), measure the $\widetilde{V}^c_L(\mathcal{P})$ for paths $\mathcal{P}$ between the ground state and it's chiral mirror image $\{-q_i\}$

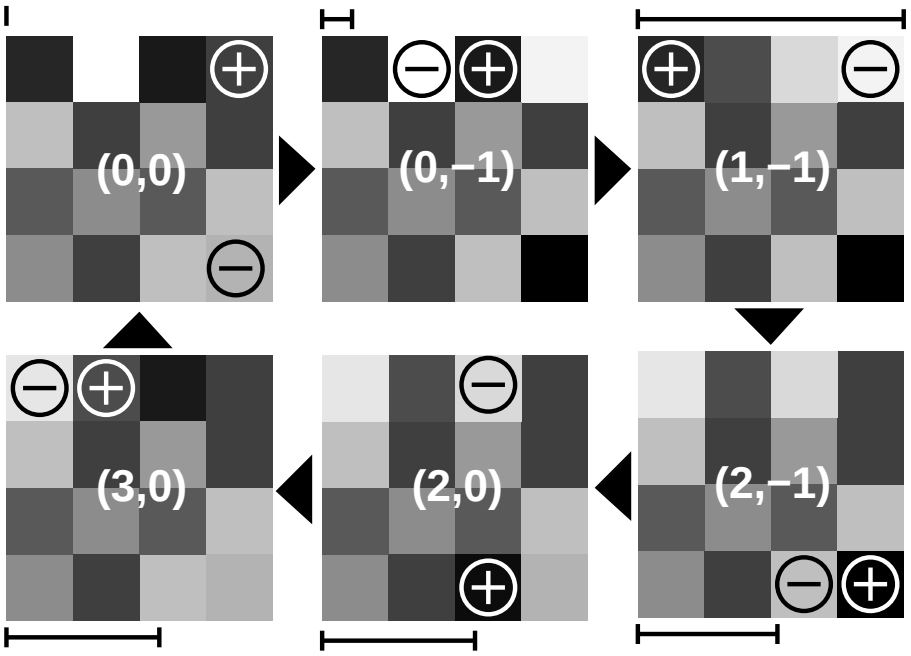

Figure 5.2: *Illustration of a complete path $\mathcal{P}$ of a realization of a 4×4 gauge glass-system, corresponding to a transport of vorticity across the system. The upper left corner is the ground state. Charge is symbolized by the shading of the squares, black represents -0.67, white represents $+0.72$, and intermediate charges are proportionally grey with zero as* ▭*. The digits show the polarization relative to the ground state. The charge symbols represent the dipole excited in the next step. The bar next to the square shows the energy of each configuration relative to the ground state.*

(regardless of polarization). Then let

$$V_L^c = \left[\left\langle \min_{\mathcal{P}} \widetilde{V}_L^c(\mathcal{P}) \right\rangle_{\text{gs}} \right] , \tag{5.3}$$

where $\langle \cdot \rangle_{\text{gs}}$ denotes average over the ground states of a particular disorder realization.

5.4 The Domain Wall Energy

In the Ising spin glass droplets with a boundary over which the spins are flipped are the fundamental excitations. Order remains as long as the droplets are limited in size. If the energy cost of introducing an anti-periodic boundary in the system is finite, arbitrary large droplets could form at any temperature, and hence there can be no finite temperature phase transition. Even if vortices, as excitations, have a more natural interpretation than droplets in vortex glass models (such as those defined in Chapter 3), the idea of studying the energy difference for introducing an antiperiodic boundary has been directly transferred to the vortex glass studies. To give a precise definition the *domain wall energy* (sometimes called the *defect energy*), ΔE_{dw} is:

$$\Delta E_{\text{dw}} = \left[\left| \min_{\Delta=0} E - \min_{\Delta=\pi} E \right| \right] . \tag{5.4}$$

An alternative definition is the "best twist" domain wall energy $\Delta E_{\text{dw}}^{\text{bt}}$ [27], where one of the energies is chosen as the twist space ground state:

$$\Delta E_{\text{dw}}^{\text{bt}} = \left[\min_{\Delta=\Delta_0+\pi} E - \min_{\Delta=\Delta_0} E \right] , \tag{5.5}$$

where Δ_0 gives the global twist space ground state.

Both versions of the domain wall energy are known to scale with the system size as $\Delta E_{\text{dw}} \sim L^\theta$ with $\theta < 0$. [27, 29, 30, 31] This means that the free-energy versus twist landscape is flat (as mentioned in Sect. 5.1), and hence that if there is no ergodicity breaking and no finite temperature transition. But on the other hand, there is no way of mapping out the ergodic regions of the phase space by using domain wall energy arguments, since neighboring points on the free-energy surface in the twist space can be very distant in phase space; i.e. to get between two points on the free-energy surface that are close in twist space, might involve a considerable number of dipole excitations leading through highly energetic intermediate states. In terms of vortices, the domain wall energy measures the 'roughness' of the energy landscape vortices travels in. But as mentioned in Sect. 5.1, it is guaranteed to be the relevant physical landscape for vortex motion only if one allows quantum tunneling of vortices. With no quantum tunneling there might be highly energetic (infinite, in the thermodynamic limit) intermediate states on any path in phase space.

There is also a DWE equivalent for detecting chiral order (see Sect. 5.3), this quantity also shows a power-law decay in L. [32, 33, 34, 35] The main topics

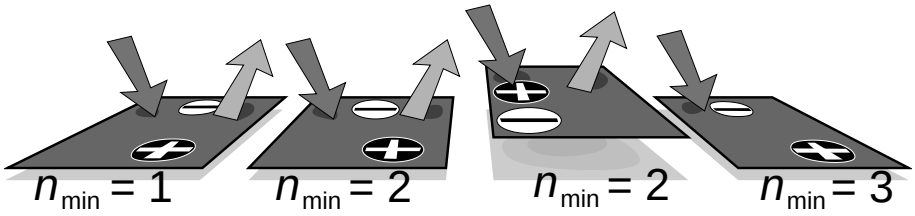

Figure 5.3: *The Spin-Quench Algorithm: The system is repeatedly heated and cooled until the lowest energy state is regenerated* $N_{\min} = 10$ *times without any other lower energy state being found.*

of the non-local-vorticity-conserving studies of XY spin glass has been whether or not the exponent for spin order θ_s and chiral order θ_c is the same. The last word so far is that $\theta_s = \theta_c$ provided that one uses the best twist boundary condition [34].

5.5 Finding the Ground State

One crucial step in zero temperature simulations is the finding of the ground state. For the gauge glass model this is close to the worst imaginable minimization problem; for the XY spin glass model things are a little bit easier. Of the many ground state finding algorithms—simulated annealing [36], entropic sampling [38], parallel tempering [39]—the standard algorithm in studies of vortex glass models has been the spin quench algorithm (SQA, introduced in Ref. [49] and refined for XY spin glass in Ref. [33]).

The idea of SQA is to repeatedly heat the system's spin and twist degrees of freedom to $T = \infty$ and relax it to $T = 0$ as fast as possible. Let $n_{\min}$ be the number of occurrences of the lowest-yet-configuration. (So, as soon as a new lowest-energy configuration $n_{\min}$ is set to zero.) When $n_{\min} = N_{\min}$ the ground state is identified as the lowest-yet-configuration.

During the cooling and heating one uses spin representation, but for comparing energy minimum configurations one transforms the system to CG representation. We choose $N_{\min} = 10$ which (in a test) for 100 disorder realizations of the largest system used, gave the same ground states as $N_{\min} = 20$, but of course one can always claim that maybe $N_{\min} = 1000$ would . . . There is anyway nothing magic with the ground state compared to other low-energetic configurations, so a small fraction of almost-ground states would hardly change the quantities in question.

The SQA is considered reliable for finding the ground state but have the significant disadvantage of being an $O(\exp L)$ algorithm and hence restricts the user to very small L. However, when V_L is the targeted quantity, the slowness of SQA does not matter much since the algorithm for finding V_L also is $O(\exp L)$.

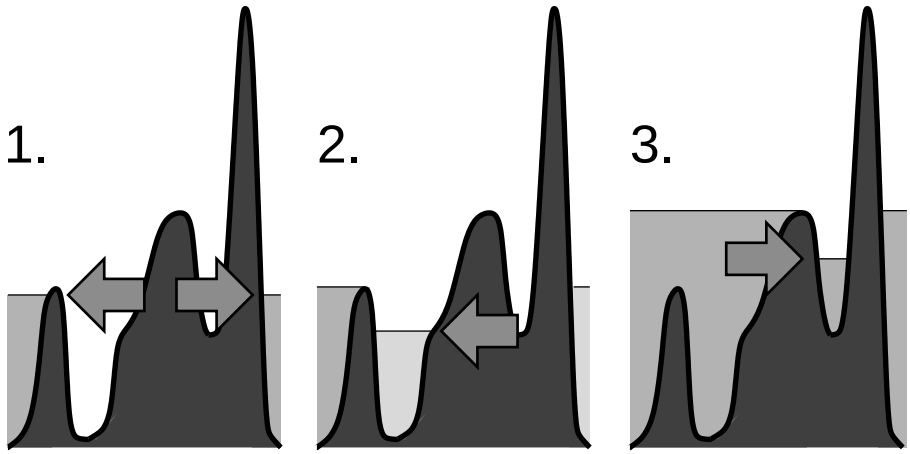

Figure 5.4: *Illustration of the flooding algorithm for finding the lowest energy barrier for vortex dissipation. The least energetic accessible configuration is investigated in the next step. The arrow shows the active energy level in the execution. The horizontal axis represents the L^2-dimensional phase space. The landscape is periodic in polarization, which is illustrated by the water level being the same at the left and right boundaries.*

5.6 Measuring the Domain Wall Energy

For finding the domain wall energy the usual method (used in e.g. Refs. [27, 31, 34]) is based on SQA. The only difference is that to get the lowest energies of a certain twist (as in Eqs. (5.4) and (5.5)) one keeps the twist degrees of freedom constant during the heating and quenching.

Other, faster algorithms has also been used [16, 30, 35] only to confirm that $\theta < 0$.

5.7 Finding the Energy Barrier for Vortex Dissipation

At a first thought, the vastness of the phase space would seem to make the tracking of a $\widetilde{V}_L(\mathcal{P}) = \widetilde{V}_L$ (see Sect. 5.2) path computationally intractable. But it turns out that the number of configurations with an energy above the ground state is not too large ($O(\exp L)$) for at least some very small system sizes. The algorithm we used may be called the *flooding algorithm* for reasons seen in Fig. 5.4: It imitates the pouring of water into a landscape, the lowest water level being the current energy level in the execution of the program.

To be precise, we start from the ground state and repeat the following steps:

1. Generate $4L^2$ configurations by applying the $4L^2$ possible dipole excitations to the current configuration.

2. Calculate the energy of each such configuration and put them in a sorted list, lowest energy first, together with their polarization relative to the ground state.

3. Take the first (lowest energy) configuration from this list to be the new current configuration.

4. If this configuration has already been encountered, but with a different polarization such that $\Delta P = (\pm L, 0)$ then we are done. Otherwise, go to step 1.

To avoid loops in the path (which would stall the execution) one also needs a list of already used configurations so that these can be rejected in step 3. When the iteration has stopped the highest energy used in step 3 is exactly V_L plus the ground state energy.

Chapter 6

Finite Temperature Methods

Zero temperature simulations have a very concrete objects to study—the ground state and its low-order excitations. Reality, on the other hand, is blurred by temperature fluctuations. This chapter will deal with finite temperature Monte Carlo methods. I will discuss the validity of Monte Carlo methods when replica symmetry is broken and the overlap (see Sect 4.2) does not have a clear meaning. In the last two sections I will give a brief introduction to a short topic that don't quite fit under the Chapter's title: the Kosterlitz-Thouless Transition (Sect. 6.3).

Throughout this Chapter I use the terminology of spin models, such as the random gauge XY model. It can all be modified for lattice gas models, but I stick to the spin picture to keep it simple (and because Paper 2 concerns a spin model, the random gauge XY model).

6.1 Metropolis Monte Carlo

The Metropolis Monte Carlo simulations technique has the darkest of origins as being developed in course of the American H-bomb program [40], but has been turned into an essential instrument of pinnacle of human achievement—the study of phase transitions in superconductors . . .

The Metropolis Monte Carlo algorithm is a way of generating configurations, so that the probability of a configuration $\{\theta_i, \Delta\}$ is proportional to $\exp(-E(\{\theta_i, \Delta\})/k_B T)$ in accordance with the Boltzmann distribution ($E(\,\cdot\,)$ denotes the energy). For the lattices we are using, one *Monte Carlo sweep* is the following steps executed for each site of the lattice once and only once:

1. For a spin θ_i, produce a new spin $\theta_i' = \theta_i + \eta$, where η is a random variable with a distribution symmetric around zero. Different η-distributions might affect the efficiency of the algorithm but will not change the statistical output as long as they are symmetric around zero.

2. Let E' be the energy of the configuration with θ_i replaced by θ_i' and let E be the energy of the original configuration. Then replace θ_i by θ_i' if $E' \leqslant E$, or with a probability $\exp[(E - E')/k_B T]$ if $E' > E$.

For the typical square grid geometry one can choose the lattice points sequentially.

Even if the distribution of configurations follow the Boltzmann distribution at every intermediate step one often runs at least one whole sweep before measuring quantities. This is because if the quantities are too correlated, one need unnecessarily large averages to converge them.

If one uses the fluctuating twist boundary condition (see Sect. 3.7) one also needs to update the twist $\Delta = (\Delta_x, \Delta_y)$. This procedure is exactly similar to the one above. To optimize the twist updating one can choose to split Δ_x (Δ_y) into L variables $\Delta_x^{(i)}$ (i.e. $\Delta_x = \sum_{i=1}^{L} \Delta_x^{(i)}$) where i is the column (row) number.

6.2 The Helicity and Fourth Order Moduli

The helicity modulus Υ (defined in Eq. (5.1)) is the most important quantity for detecting a normal to superconducting transition in the XY type of models. Υ is zero in the normal phase and finite when the system is superconducting. As such it fulfills the requirements for being a order parameter of the XY model, but it is a non-local quantity as opposed to e.g. magnetization—the order parameter of the Ising model. (See Sect. 4.2.)

In simulations, a singular behavior at a phase transition, is always smeared by finite size effects. The transition is often more clearly visible in a higher order derivative of a singular quantity. One of the most well known examples is C_V, the temperature derivative of the energy, with is effective in localizing first order transitions. We use the second derivative of Υ, the *fourth order modulus* Υ_4, see Fig. 6.1. (The third order derivative is zero by symmetry.) To get a feeling for Υ_4 one can write it as a sum of correlation terms for lower order quantities, and compare with corresponding quantities for the first two terms in the Δ-expansion of F:

$$I \equiv \frac{\partial F}{\partial \Delta} = \langle \widehat{I} \rangle_{\rm re} = \left\langle \frac{1}{L} \sum_{(ij)^x_{\rm nn}} \sin \phi_{ij} \right\rangle_{\rm re} \tag{6.1}$$

$$\Upsilon \equiv \frac{\partial^2 F}{\partial \Delta^2} = \langle \widehat{\Upsilon} \rangle_{\rm re} = \left\langle -\widehat{E} - \frac{1}{T}(\widehat{I} - I)^2 \right\rangle_{\rm re} \tag{6.2}$$

$$\Upsilon_4 \equiv \frac{\partial^4 F}{\partial \Delta^4} = \left\langle -4\Upsilon - 3E - \frac{3L^2}{T}(\widehat{\Upsilon} - \Upsilon)^2 + \frac{2}{L^2 T^3}(\widehat{I} - I)^4 \right\rangle_{\rm re} \tag{6.3}$$

where hats mark values for one $\{\phi_{ij}\}$ configuration, the summation is over all links in the x direction, and $\widehat{E} = -(1/L^2) \sum_{(ij)^x_{\rm nn}} \cos \phi_{ij}$. The advantage of writing Υ_4 as in Eq. (6.3) is that it becomes a sum of quantities with a clear interpretation, e.g. $(2/L^2T^3)(\widehat{I} - I)^4$ measures the fluctuations in current and is zero in the thermodynamic limit for periodic and fluctuating twist boundary conditions.

For readers who want to measure Υ and Υ_4 in simulations, I give Eqs. (6.2) and (6.3) rewritten in explicit sums of cosine and sine:

$$\Upsilon = \frac{1}{L^2} \langle \cos \rangle - \frac{1}{L^2 T} \langle \sin^2 \rangle + \frac{1}{L^2 T} \langle \sin \rangle^2 \tag{6.4}$$

$$\Upsilon_4 = -\frac{1}{L^2} \langle \cos \rangle + \frac{4}{L^2 T} \langle \sin^2 \rangle - \frac{3}{L^2 T} \langle \cos^2 \rangle - \frac{4}{L^2 T} \langle \sin \rangle^2 + \frac{3}{L^2 T} \langle \cos \rangle^2 +$$

$$+\frac{6}{L^2T}\langle\sin^2\cos\rangle-\frac{12}{L^2T^2}\langle\sin\rangle\langle\sin\cos\rangle+\frac{12}{L^2T^2}\langle\sin\rangle^2\langle\cos\rangle-$$
$$-\frac{6}{L^2T^2}\langle\cos\rangle\langle\sin^2\rangle-\frac{1}{L^2T^3}\langle\sin^4\rangle+\frac{4}{L^2T^3}\langle\sin\rangle\langle\sin^3\rangle-$$
$$-\frac{12}{L^2T^3}\langle\sin\rangle^2\langle\sin^2\rangle+\frac{3}{L^2T^3}\langle\sin^2\rangle^2+\frac{6}{L^2T^3}\langle\sin\rangle^4 \tag{6.5}$$

where for example $\langle\sin^2\cos\rangle=\left\langle(\Sigma_{\langle ij\rangle_{\rm nn}}\sin\phi_{ij})^2\,\Sigma_{\langle ij\rangle_{\rm nn}}\cos\phi_{ij}\right\rangle_{\rm re}$, and the sums are taken in a certain direction x or y (for symmetric systems one can use $\Upsilon=\Upsilon_x=\Upsilon_y=(\Upsilon_x+\Upsilon_y)/2$ to get better averages).

6.3 The Kosterlitz-Thouless Transition

The transition in the ordinary 2D XY model is called the Kosterlitz-Thouless (KT) transition [41], and occurs at $T_{\rm KT}\approx 0.89$. The low-temperature phase is characterized by vortices bound in pairs and an algebraic decay of spin correlations, so called *quasi long range order*. The way to explain the pair-binding is that the energy for introducing one single vortex to the ground state grows unboundedly with system size (as $\log L$), whereas the energy for introducing a pair is finite. For higher temperatures the vortex interaction becomes screened by other vortices, the infinite energy for a free vortex will then vanish. A proper renormalization group treatment confirms this idea. [45] Under the assumptions of the domain wall energy*, a domain wall renormalization group study [46] shows that there is an upper limit for the disorder $r>r_c\approx 0.4$ in the random gauge XY model above which there can be no finite temperature phase of the same characteristics as the low-T phase of the ordinary XY model [47].

The fourth order modulus is never positive for the ordinary XY model. It is zero for high temperatures (this is a necessity since it is defined around a minimum of F, and $\Upsilon=0$), and approaches -1 as $T\to 0$, while it diverges at $T_{\rm KT}$. For the standard XY model one knows how $\Upsilon(T_{\rm KT})$ scales with L [42], so to study Υ_4 (that is harder to converge) adds nothing of much value. But to detect an unknown phase transition, the onset of strong size-dependence of Υ_4 close to T_c (see Fig. 6.1) can be utilized.

6.4 Root-Mean-Square Current

The helicity modulus is hard to converge due to the strong current fluctuations from sample to sample [43]. On the other hand, the current fluctuations are expected to diverge at T_c, so in order to pick up that divergence Ref. [44] has studied the root-mean-square current $I_{\rm rms}$ with periodic boundary conditions:

$$I_{\rm rms}=\sqrt{[I^2]}\,, \tag{6.6}$$

where I is defined in Eq. (6.1).

*I.e. that intermediate configurations does not have any bearing on the vortex dynamics (see Sect. 5.4).

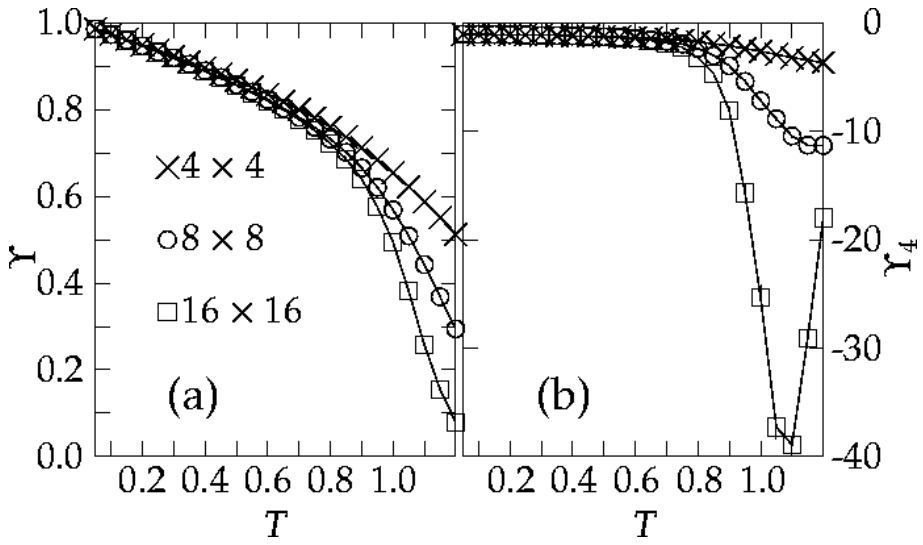

Figure 6.1: *The Kosterlitz-Thouless transition at* $T_{\mathrm{KT}} \approx 0.89$ *as seen through the quantities* Υ *(a) and* Υ_4 *(b).*

I_{rms} has been used to argue for a zero-T transition [44] on the basis of the apparent lack of crossing point in Fig. 6.2a. Figure 6.2b shows the more extensive recent simulations from Paper 2 which shows that the $T_c = 0$ scaling fails (the curves do not converge to a single curve as $T \to 0$). Figure 6.3 shows that the same scaling form that gives Υ a unique crossing point (see Paper 2) also makes the I_{rms} cross at one point. This scaling makes the I_{rms} curves (see Fig. 6.3b) cross at the same point as the Υ-curves, at $T \approx 0.2$—a clear evidence for a phase transition. This is of course a great example of researchers that see what they want to see (which is true both for Young and myself).

6.5 The Pitfalls of Vortex Glass Monte Carlo

When there is a possibility of replica symmetry breaking in systems with a local order parameter (such as the Ising spin glass of Sect. 4.2) the overlap function gives a way around slow physical dynamics and hand-waving argumentation. With an overlap function, we can sample the system according to the Boltzmann distribution, and get information about the type of order in the low temperature phase and the expectation values of physical quantities. Without a local order parameter, which is probably the case in our vortex glass models, we can of course calculate the overlap of local quantities. That would give us the probability distribution of these quantities, but nothing more.

So, what can we do without the overlap technique if replica symmetry breaking occurs? We can of course go on like nothing has happened and use the time averages, as long as we don't violate the physical dynamics (which we specify to be local vorticity conservation) when we update the system. If we do so, the next problem is how long we should run the simulations to get true physical values. For answering this question we have to consider two cases—whether or not the system is disorder self-averaging: If the system is disorder

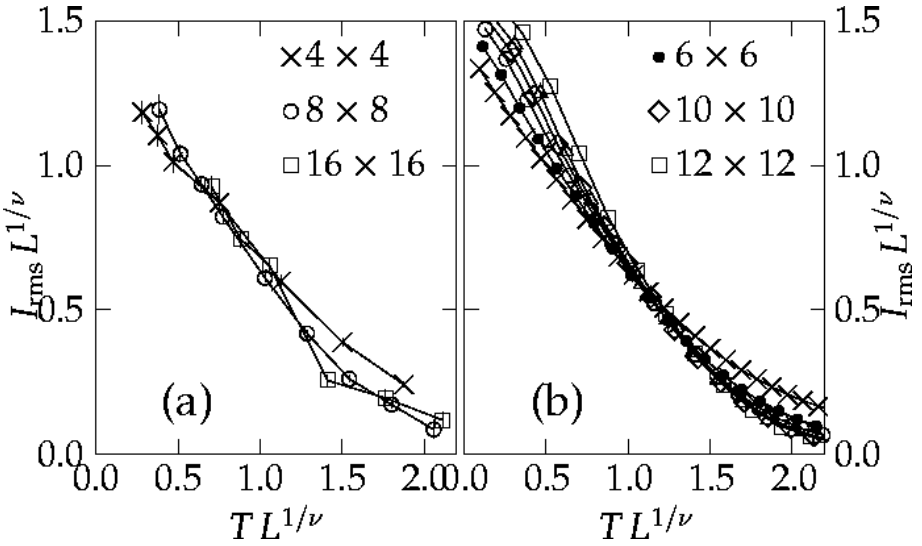

Figure 6.2: *(a) and (b) shows a crossing plot of $I_{\rm rms}$ according to the scaling form of Young [44], (a) is Young's original data, (b) is our data. In both (a) and (b) $\nu = 2.2$.*

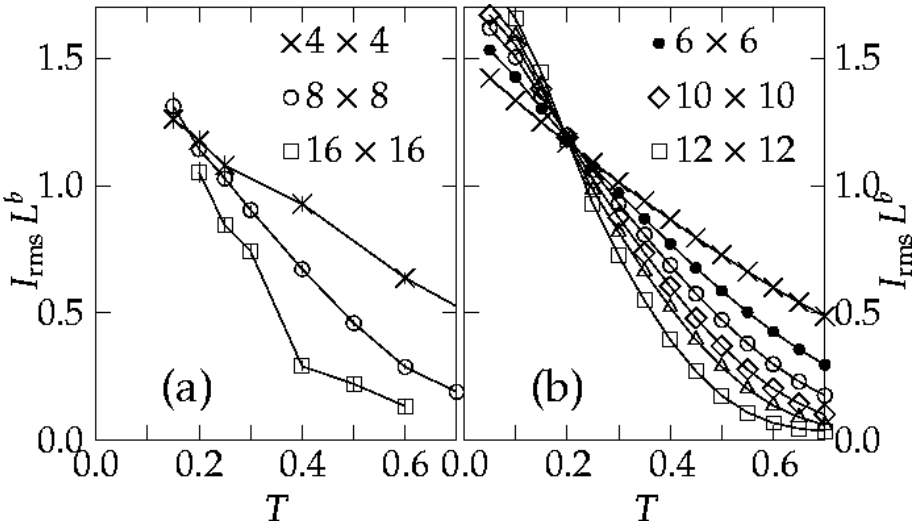

Figure 6.3: *The $I_{\rm rms}$ data plotted according to our scaling form. (a) is Young's original data, (b) is our data. In both (a) and (b) $b = 0.5$. A collapse plot corresponding to (b) can be found in paper 2.*

self-averaging with respect to the quantities we are interested in, then we can continue just like for a model without disorder. When curves look smooth, and crossing and collapse plots looks clear and convincing, we can trust the results. (A discussion about this can be found in Ref. [23].) To go one step further one can argue that if one can e.g. produce a distinct crossing plot according to the standard finite-scaling hypothesis then the system is likely to be disorder self-averaging. But if the system isn't disorder self-averaging the situation is worse, as two independent measurements could give different results.

When local quantities, such as magnetization, not are disorder self-averaging locally, then at least their average value are. [19] But for global quantities such as Υ and Υ_4 this argument doesn't apply. So is it likely that a low-temperature phase with replica symmetry breaking in our vortex glass models is not disorder self-averaging with respect to Υ and Υ_4? As mentioned in Sect. 5.1 the curvature of the free-energy versus twist landscape is probably the same in a neighborhood of every minimum, and neighborhoods might be of finite size due to the ergodicity breaking. From this, one can guess that the system is disorder self-averaging with respect to Υ and Υ_4, at least at the lowest temperatures (there is also a possibility that the system freezes into different minima at different temperatures). So if Υ scales to a non-zero value for temperatures very close to zero, then is quite safe to say that the same would happen in the thermodynamic limit. To trust the T_c and exponents obtained from finite-size scaling one has to be a little more brave, though.

If one studies an overlap function, such as in Ising spin glass one wants to update the system in such a way that one avoids getting stuck in a confined part of phase space. There are methods to do that by being able to jump between different energy valleys (e.g. entropic sampling [38]) and still sample the phase space according to the Boltzmann distribution. But as soon as one wants to measure a quantity which is dependent on a symmetry that can break in a phase transition, these methods will give unphysical results. The only solution left is then to sample the system with the physical dynamics. [23] As an example, the average magnetization in the Ising model is zero for every temperature if one assumes ergodicity and neglects the physical dynamics (a finite number of spin-flips at each time step).

6.6 Annealing Conditions and the Best Twist Boundary Condition

If one, according to Sect. 6.5 chooses to update the system with physical dynamics and measure time averages, then how slow should one cool the system? One plausible choice, for the reasons to follow, is to aim for the most probable region of the phase space:[†] 1. It is relatively easy to identify, since as long as the system is ergodic it is most likely to be close to this minimum. Unfortunately, to measure distance in the phase space is very hard, so one can make the usual projection to twist space, hope that one doesn't oversimplify the problem, and look for the most probable twist space coordinates. 2. It is easy to check if the

[†]The most probable configuration will also be the global energy minimum as long as the system is ergodic. But if one anneals the system it is most likely to freeze into the least energetic of the regions that will be the isolated ergodic regions when ergodicity is broken.

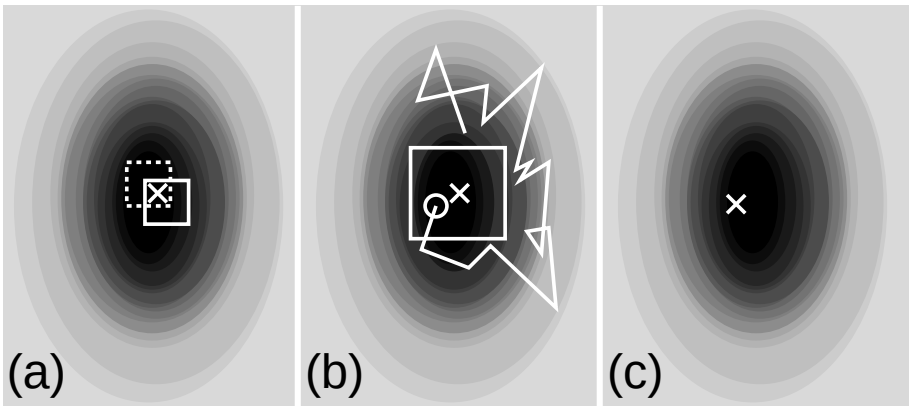

Figure 6.4: *Illustration of the annealing algorithm. Dark color represents large value of the histogram:* ***(a)*** *First two replicas of the system are cooled and two* $(\widehat{\Delta}_x, \widehat{\Delta}_y)$ *obtained, if these are close enough (if the two squares with a side* ϵ *overlap) the average* $(\widehat{\Delta}_x, \widehat{\Delta}_y)$*, the '*$\times$*', is fixed.* ***(b)*** *Then one lets the program run until the twist comes close enough (within the square with side* 2ϵ*) to* $(\widehat{\Delta}_x, \widehat{\Delta}_y)$*.* ***(c)*** *At last one fixes* $(\widehat{\Delta}_x, \widehat{\Delta}_y)$ *to that of the last configuration and continues to update only the spin variables while measuring quantities.*

cooling is slow enough—if the system is far off the most popular twist-space coordinates. 3. Quantities like Υ and Υ_4 are well defined around the minimum of the ergodic region of the phase space in which the system is. To be able to study these quantities around a minimum one wants a minimum that is as distinct as possible, and that is something that the global minimum is likely to be.

The mostly used way to avoid getting stuck in a meta-stable part of phase space when one cools the system, is an *annealing condition* to check that cooling is slow enough. The idea, originating for the study of Ising spin glass [36], is to cool two copies (or *replicas*) of the system in parallel. Then one measures the time average for some quantity, e.g. the spin-glass susceptibility:

$$\chi_{\mathrm{SG}} = \frac{1}{L^2} \sum_{ij} \langle s_i s_j \rangle_t^2 \tag{6.7}$$

for both replicas, and when these two values are sufficiently converged the cooling is said to be slow enough. To be sure that the algorithm not only calculates the correct values for some quantity, but also stays close to the most probable minimum one can modify the annealing condition. The way to do it is to use FTBC and make a histogram of Δ. The peak of the histograms $(\widehat{\Delta}_x, \widehat{\Delta}_y)$ will correspond to the most probable minimum. To check that the cooling is slow enough one can use the replica technique and for each temperature cool the system twice to obtain two values of $(\widehat{\Delta}_x, \widehat{\Delta}_y)$, say $(\widehat{\Delta}_x^{(1)}, \widehat{\Delta}_y^{(1)})$ and $(\widehat{\Delta}_x^{(2)}, \widehat{\Delta}_y^{(2)})$. Then, if the condition

$$|\widehat{\Delta}_x^{(1)} - \widehat{\Delta}_x^{(2)}| < \epsilon \text{ and } |\widehat{\Delta}_y^{(1)} - \widehat{\Delta}_y^{(2)}| < \epsilon, \tag{6.8}$$

fails,[‡] one can redo the cooling with (say) three times as many thermalization sweeps, and repeat the procedure again, until the condition (6.8) is fulfilled. To maximize the possibility of finding the correct ground state for every new temperature, one can begin the thermalization from a configuration satisfying (6.8), see Fig. 6.4. Of course, twist space is only a two-dimensional projection of the phase space, so that the twist space coordinates are close to the peak of the histograms does not necessarily mean that the configuration is close, in terms of dipole excitations, to the ground state. But this is probably the best way to do without tedious vortex movement calculations as those described in Chapter 5. In an attempt to justify this algorithm *a posteriori* I have compared the results of this annealing algorithm with SQA (see Sect. 5.5) for 100 disorder realizations of 5×5 gauge glass systems, and the two algorithms found the same ground state for every disorder.[§]

Quantities such as the helicity and fourth order moduli (see Sect. 6.2) cannot be determined with very high precision if FTBC is used, therefore after determining the $(\widehat{\Delta}_x, \widehat{\Delta}_y)$ one can fix this twist and continue the Monte Carlo scheme with only spin variable updating. To calculate quantities starting from the global twist space ground state is similar to the definition of the best twist version of the domain wall energy in Sect. 5.4, thus the name *best twist boundary condition* (BTBC).

[‡]In practice a sensible choice of ϵ, for the random gauge XY model, seems to be $\epsilon = 0.3$ for $0.4 < T \leqslant 0.6$ and $\epsilon = 0.09$ for $T \leqslant 0.4$.

[§]This result should not be taken too seriously since the energy landscape of a 5×5 is far less complex than the largest tractable sizes for the annealing algorithm in question.

Chapter 7

Summary of the Papers

Much of the ideas in the papers have already been presented in the first four chapters of this Thesis. In this Chapter I will link the discussions in the earlier part of this Thesis with the papers, and also link the Thesis with experimental and other theoretical studies.

7.1 Paper 1

In this paper we measure the barrier for vortex dissipation V_L, presented in Section 5.2, of the models presented in Sections 3.3, 3.4, and 3.5.

For the random gauge XY model we find a logarithmically increasing V_L with an abrupt change in the prefactor at disorder strength $r \approx 0.4$—for $r > 0.4$ the slope is almost constant. This is interpreted as a phase line between two superconducting phases: A phase characterized by pair-bound vortices, for small r; and phase where replica symmetry is broken for large r. There are, as mentioned, some assumptions made in the generalization from zero to finite temperature, but at the very least we can say that there is no way measurements of V_L or ΔE_{dw} (see Sect. 5.4) can exclude a low temperature phase for all strengths of the disorder, unless one assumes quantum tunneling of vortices to be possible.* The phase diagram is shown in Fig. 7.1, values (other than r_c) are obtained by Monte Carlo methods.

For the XY spin glass model we find V_L to be independent of L for all measured values of the disorder density s. This means that there can be no spin ordered phase in the XY spin glass model. An interesting question for future studies is a better determination of the critical disorder density s_c (remember that $s = 0$ is the ordinary XY model with a low-T phase of quasi long-range spin order). We also found that the barrier for chiral order (see Section 5.3) increases for all measured values of s, implying a possible chirally ordered phase. As for spin order we did not make a detailed determination of the critical disorder density for the chiral barrier s_c^c; the best we can say is that $0 \leqslant s_c, s_c^c < 0.1$.

For the random pinning model we found a decreasing V_L. This means that there is no barrier stopping vortex dissipation in this model. Since the random pinning model is believed to be the most physical model for thin films in external magnetic fields, our best bet is that there is no superconducting phase in

*If quantum tunneling of vortices is possible DWE studies shows that $T_c = 0$ for $r > r_c$.

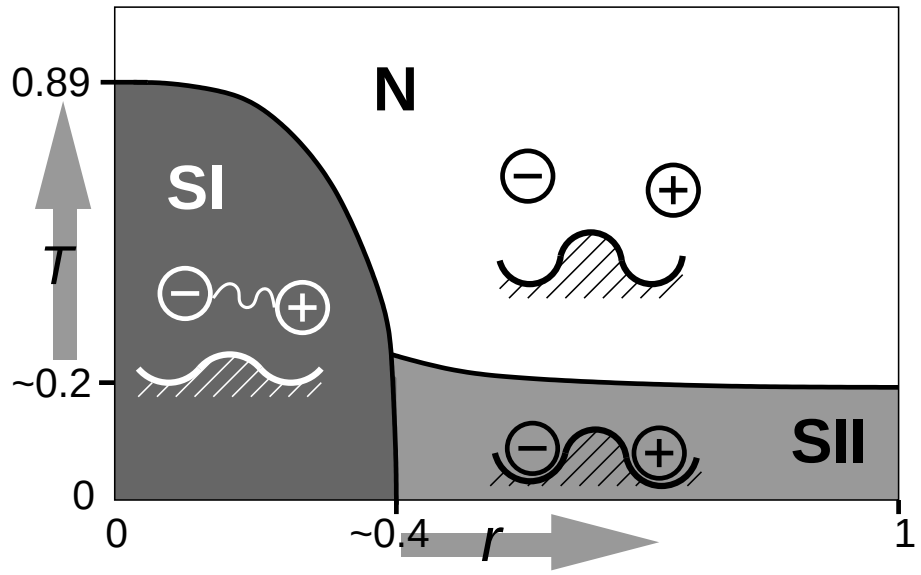

Figure 7.1: *The phase diagram of the random gauge XY model. 'N' is the normal conducting phase, 'SI' is a superconducting phase where vortices are bound in pairs, 'SII' is a superconducting phase where replica symmetry is broken. The illustration of the SII phase is not to be taken too seriously.*

this case.

7.2 Paper 2

In this paper we try to map out the phase diagram, suggested by the first paper, by finite temperature Monte Carlo with the BTBC annealing described in Section 6.6.[†] (See Fig. 7.1.)

For the N-SII transition we perform a finite-size scaling analysis to get $T_c \approx 0.19$ for the gauge glass model ($r = 1$). For r between 0.4 and 1.0 increasing disorder strength does not make any major difference—just as seen in the zero temperature studies for the slope of $\exp V_L$—the transition temperature stays around 0.2.

With extended I_{rms}-simulations we find that the old arguments for a zero temperature transition fails, and that I_{rms} gives roughly the same values for T_c and the exponents ν and b as the helicity modulus scaling.

As mentioned in Sections 4.3 and 6.5, even if there is replica symmetry breaking at low temperatures the helicity modulus is probably disorder self-averaging, which would save our finite scaling analysis. If Υ not is disorder self-averaging our study at least shows that a realization of an experiment would most likely show existence of a superconducting phase at finite temperatures.

For the N-SI and SI-SII transition we measure the fourth order modulus (see Section 6.2), and locate the transitions lines to the points of strong size dependence of this quantity.

[†]Well, actually the two papers were produced quite independently of each other.

7.3 Conclusions

The random gauge XY model has a low-temperature superconducting phase for all disorder strengths, and replica symmetry is broken at low temperatures for $r > r_c$. The spin correlations of the SII phase is an open question, it is known that there can be no long-range glass order [5] in the gauge glass model (but remember that the ordinary XY model only have quasi long range order). From Monte Carlo simulations we estimate $T_c \approx 0.2$ for $0.4 \lesssim r \leqslant 1$ and T_c decreasing from 0.89 to 0.2 for $0 \leqslant r \lesssim 0.4$.

The apparently contradictory results for the random gauge XY model (where Refs. [25, 50, 51] argue for and Refs. [16, 27, 28, 29, 30, 31, 33, 44] against a finite temperature transition) is thus a question of dynamics and what transition to look for: Refs. [16, 27, 28, 29, 30, 31, 33, 44] shows that there is no transition to a phase with long-range glass order, and that there can be no superconducting phase if vortex tunneling dynamics are allowed. Refs. [25, 50, 51] shows that with local vorticity conserving dynamics there exists a low-temperature phase for values of the disorder strength.

The scaling of Υ_4 (see Paper 2), the prefactor of V_L (see Paper 1) and Ref. [47] all suggests a phase boundary at $r \approx 0.4$, but with Figure 5.1 in mind one may wonder if there really is any qualitative difference between the high-r and low-r phases. One clear difference is that continuous vortex motion is a likely way of vorticity transport for low r, whereas for large r multiple dipole excitations must, from energetic judgment, be the predominant mode for vorticity transport (Fig. 5.2 illustrates multi vortex hopping giving a lowest energetic path).[‡] But we cannot be absolutely sure that the phase space is partitioned in the way suggested by Figure 5.1—so that the free-energy versus twist landscape consists of one parable for each polarization space coordinate. But we can say that there are intermediate energy barriers that seems to scale to infinity (from the scaling of V_L), and that the curvature of the energy landscape around the valleys is high (from the scaling of Υ).

Does the finite temperature transition for every r of the random gauge XY model support the finding of a thin-film vortex glass phase in Ref. [10]? Well, Ref. [10] assumes the standard vortex glass scaling (used in Fig. 6.2). This is wrong in the first place, since it is based on the assumption of a low-T phase with long range glass order (which cannot exist in two dimensions [5]); furthermore it is not the scaling form we find (see Fig. 6.2 and Paper 2). Since the apparently most physical vortex glass model, the random pinning model, has a decaying barrier for vortex dissipation the conclusion must, in accordance to the larger part of the experimental community [9], be that no superconducting phase can exist for strongly disordered thin films.

[‡]Some effort has also been done to understand the difference of SI and SII in terms of spin correlations. These results, although preliminary, supports the picture suggested in Fig. 7.1: In the SI phase, just like the ordinary XY model, is characterized by pair-bound vortices and algebraically decaying spin-correlations—the vortex-vortex interaction overrides the disorder. In the SII phase disorder becomes relevant and correlations has to be calculated relative to disorder, as has been done in the pro-$T_c > 0$ article Ref. [51].

Bibliography

[1] The archaeologically interested might want to dig up: H. Kammerlingh Onnes, Akad. van Wetenschappen **14**, 818 (1911). W. Meissner and R. Ochsenfeldt, Naturwissenschaften **21**, 787 (1933).

[2] For general introductions to superconductivity, see e.g. the rather advanced: M. Tinkham, *Introduction to Superconductivity*, (McGraw-Hill, New York, 1975); or the more basic: M. Cyrot and D. Pavuna, *Introduction to superconductivity and high-T_c materials*, (World Scientific, Singapore, 1992).

[3] Cuprate high-T_c superconductors should be well known to the physical community, but it all started with: J. G. Bednorz and K. A. Müller, Z. Phys. **64**, 189 (1986).

[4] A. A. Abrikosov, Zh. Eksp. Teor. Fiz. **32**, 1442 (1957) [Sov. Phys. JETP **5**, 1174 (1975)].

[5] H. Nishimori, Physica A **205**, 1 (1994).

[6] Other phases includes the "Bragg glass phase": T. Giamarchi and P. Le Doussal, Phys. Rev. Lett. **72**, 1530 (1994); T. Giamarchi and P. Le Doussal, Phys. Rev. B **52**, 1242 (1995); M. J. P. Gingras and D. A. Huse, Phys. Rev. B **53**, 15193 (1996); D. Ertaş and D. R. Nelson, Physica C **272**, 79 (1996); J. Kierfield *et al.*, Phys. Rev. B **55**, 626 (1997); T. Giamarchi and P. Le Doussal, Phys. Rev. B **55**, 6577 (1997); S. Ryu *et al.*, Phys. Rev. Lett. **77**, 2300 (1996); A. van Otterlo *et al.*, Phys. Rev. Lett. **81**, 1497 (1998); C. J. Olson *et al.*, Phys. Rev. Lett. **85**, 5416 (2000); R. Sugano *et al.*, Physica B **284-288**, 803 (2000); R. Sugano *et al.*, Physica C **341-348**, 1113 (2000); and the "vortex slush phase": T. K. Worthington *et al.*, Phys. Rev. B **46**, 11854 (1992); D. T. Fuchs *et al.*, Phys. Rev. Lett. **80**, 4971 (1998); T. Blasius *et al.*, Phys. Rev. Lett. **82**, 4926 (1999); K. Kimura *et al.*, J. Low Temp. Phys. **117**, 1471 (1999); K. Kimura *et al.*, Physica B **284-288**, 717 (2000). T. Nishizaki *et al.*, Physica C **341-348**, 957 (2000).

[7] M. P. A. Fisher, Phys. Rev. Lett. **62**, 1415 (1989); D. S. Fisher, M. P. A. Fisher, and D. A. Huse, Phys. Rev. B **43**, 130 (1991).

[8] R. H. Koch *et al.*, Phys. Rev. Lett. **63**, 1511 (1989); R. H. Koch, V. Foglietti, and M. P. A. Fisher, Phys. Rev. Lett. **64**, 2586 (1990); P. L. Gammel, L. F. Schneemeyer, and D. J. Bishop, Phys. Rev. Lett. **66**, 953 (1991); T. K. Worthington *et al.*, Phys. Rev. B **43**, 10539 (1991); H. K. Olsson *et al.*,

Phys. Rev. Lett. **66**, 2661 (1991); P. Voss-de Haan, G. Jacob, and H. Adrian, Phys. Rev. B **60**, 12443 (1999),

[9] C. Dekker, W. Eidelloth, and R. H. Koch, Phys. Rev. Lett. **68**, 3347 (1992); C. Dekker *et al.*, Phys. Rev. Lett. **69**, (1992) 2717; E. Sandvold and C. Rossel, Physica C **190**, 309 (1992); Q. Li *et al.*, Phys. Rev. B **50**, 4256 (1994); H. Yamasaki *et al.*, Phys. Rev. B **50**, 12959 (1994); Q. Li *et al.*, Appl. Phys. Lett. **66**, 637 (1995); P. J. M. Wöltgens *et al.*, Phys. Rev. B **52**, 4536 (1995).

[10] A. Sawa *et al.*, Phys. Rev. B **58**, 2868 (1998).

[11] V. L. Ginzburg and L. D. Landau, Zh. Eksp. Teor. Fiz. **20**, 1064 (1950).

[12] P. Olsson, *Vortex Fluctuations in Superconductors*, (Ph.D. Thesis, Umeå University, 1992).

[13] For a review on non-disordered two-dimensional superconductors, see: P. Minnhagen, Rev. Mod. Phys. **59**, 1001 (1987).

[14] J. Villain, J. Phys. C **10**, 1717 (1977).

[15] J. V. José *et al.*, Phys. Rev. B **16**, 1217 (1977).

[16] R. A. Hyman *et al.*, Phys. Rev. B **51**, 15304 (1995).

[17] H. Kawamura and M. Tanemura, J. Phys. Soc. Jpn. **60**, 608 (1991); H. Kawamura, Phys. Rev. B **51**, 12398 (1995); C. Wengel and A. P. Young, Phys. Rev. B **54**, 6868 (1996); H. Kawamura and M. S. Li, Phys. Rev. Lett. **78**, 1556 (1997); H. Kawamura and M. S. Li, J. Phys. Soc. Jpn. **66**, 2110 (1997); J. Kisker and H. Rieger, Phys. Rev. B **58**, 8873 (1998).

[18] P. Olsson, Phys. Rev. B **46**, 14598 (1992); A. Vallat and H. Beck, Phys. Rev. B **50**, 4015 (1994); P. Olsson, Phys. Rev. B **52**, 4511 (1995); B. J. Kim, P. Minnhagen, and P. Olsson, Phys. Rev. B **59**, 11506 (1999).

[19] N. Goldenfeld, *Lectures on Phase Transitions and the Renormalization Group*, (Perseus, Reading, 1992).

[20] K. Binder and A. P. Young, Rev. Mod. Phys. **58**, 801 (1986); M. Mézard, G. Parisi, and M. A. Virasoro, *Spin Glass Theory and Beyond* (World Scientific, Singapore, 1987).

[21] The idea of replica symmetry breaking was introduced in: A. Blandin, J. Phys. Colloq. **C6-39**, 1499 (1978); and further developed in: G. Parisi, Phys. Rev. Lett. **43**, 1754 (1979); G. Parisi, J. Phys. A **13**, L155 (1980); G. Parisi, J. Phys. A **13**, 1101 (1980); G. Parisi, J. Phys. A **13**, 1887 (1980); G. Parisi, Phys. Rev. Lett. **50**, 1946 (1983).

[22] J. Reger, R. Bhatt, and A. P. Young, Phys. Rev. Lett. **64**, 1859 (1990); A. Georges, M. Mézard, and J. S. Yedidia, Phys. Rev. Lett. **64**, 2937 (1990); N. E. Israeloff, G. B. Alers, and M. B. Weissman, Phys. Rev. B **44**, 12613 (1991).

[23] K. Binder and D. W. Heermann, *Monte Carlo Simulation in Statistical Physics*, (Springer, Berlin, 1988).

[24] This phenomenon was first suggested by experiments in A. V. Mitin, Zh. Eksp. Teor. Fiz. **93**, 590 (1987) [Sov. Phys. JETP **66**, 335 (1987)], and later given a phenomenological model in B. I. Ivlev, Y. N. Ovchinnikov, and R. S. Thompsson, Phys. Rev. B **44**, 7023 (1991).

[25] B. J. Kim *et al.*, Phys. Rev. B **56**, 6007 (1997); B. J. Kim, Phys. Rev. B **62**, 644 (2000).

[26] Dynamical simulations of two-dimensional non-disordered superconductors is performed in: B. J. Kim, P. Minnhagen, and P. Olsson, Phys. Rev. B **59**, 11506 (1999). Dynamical simulations of 2D vortex glass models includes: Refs. [25, 16].

[27] J. M. Kosterlitz and N. Akino, Phys. Rev. Lett. **81**, 4672 (1998).

[28] M. P. A. Fisher, T. A. Tokuyasu, and A. P. Young, Phys. Rev. Lett. **66**, 2931 (1991).

[29] M. Cieplak, J. R. Banavar, and A. Khurana, J. Phys. A **3**, L145 (1991); M. Cieplak *et al.*, Phys. Rev. B **45**, 786 (1992); H. S. Bokil and A. P. Young, Phys. Rev. Lett. **74**, 3021 (1998).

[30] E. Granato, Phys. Rev. B **58**, 11161 (1998).

[31] M. J. P. Gingras, Phys. Rev. B **45**, 7547 (1992).

[32] M. A. Moore and S. Murphy, Phys. Rev. B **50**, 3450 (1994); M. Ney-Nifle and H. J. Hilhorst, Phys. Rev. B **51**, 8357 (1995); H. S. Bokil and A. P. Young, J. Phys. A **29**, L89 (1996).

[33] J. Maucourt and D. R. Grempel, Phys. Rev. Lett. **80**, 770 (1998).

[34] J. M. Kosterlitz and N. Akino, Phys. Rev. Lett. **82**, 4094 (1999).

[35] S. Jain and A. P. Young, J. Phys. C **19**, 3913 (1986); E. Granato, Phys. Rev. B **61**, 391 (2000).

[36] R. N. Bhatt and A. P. Young, Phys. Rev. B **37**, 5606 (1988).

[37] M. E. J. Newman and G. T. Barkema, *Monte Carlo Methods in Statistical Physics* (Oxford University Press, New York, 1999).

[38] J. Lee, Phys. Rev. Lett. **71**, 211 (1993). A more general description can be found in Ref. [37].

[39] K. Hukushima and K. Nemoto, J. Phys. Soc. Jpn. **65**, 1604 (1996); E. Marinari, G. Parisi, and J. J. Ruiz-Lorenzo, in *Spin Glasses and Random Fields*, edited by A. P. Young (World Scientific, Singapore, 1997); E. Marinari, in *Advances in Computer Simulation*, edited by J. Kertész and I. Kondor (Springer, Berlin, 1998); K. Hukushima, Phys. Rev. E **60**, 3606 (1999);

[40] N. Metropolis *et al.*, J. Chem. Phys. **21**, 1087 (1953). Good general texts on Monte Carlo methods in statistical physics are: Refs. [23] and [37]. For a review of Monte Carlo methods for disordered systems, see: S. Jain, *Monte Carlo Simulations of Disordered Systems*, (World Scientific, Singapore, 1992).

[41] J. M. Kosterlitz and D. J. Thouless, J. Phys. C **6**, 1181 (1973). Independently described in: V. L. Berezinskii, Zh. Eksp. Teor. Fiz. **61**, 1144 (1972) [Sov. Phys. JETP **34**, 610 (1972)].

[42] H. Weber and P. Minnhagen, Phys. Rev. B **37**, 5986 (1988).

[43] This was pointed out already in: J. D. Reger *et al.*, Phys. Rev. B **44**, 7147 (1991).

[44] A. P. Young, in *Inaugural Symposium on Random Magnetism and High Temperature Superconductivity*, edited by W. Beyerman, N. L. Huang-Liu, and D. E. MacLaughlin (World Scientific, Singapore, 1994).

[45] J. M. Kosterlitz, J. Phys. C **7**, 1046 (1974). Further developments include: J. V. José *et al.*, Phys. Rev. B **16**, 1217 (1977); A. P. Young, J. Phys. C **11**, L453 (1978); A. P. Young and T. Bohr, J. Phys. C **14**, 2713 (1981); P. Minnhagen, Phys. Rev. Lett. **54**, 2351 (1985); P. Minnhagen, Phys. Rev. B **32**, 7548 (1985).

[46] J. R. Banavar and M. Cieplak, Phys. Rev. Lett. **48**, 832 (1982); W. L. McMillan, Phys. Rev. B **29**, 4026 (1983).

[47] J. M. Kosterlitz and M. V. Simkin, Phys. Rev. Lett. **79**, 1819 (1997).

[48] M. P. A. Fisher, Phys. Rev. Lett. **62**, 1415 (1989); D. S. Fisher, M. P. A. Fisher, and D. A. Huse, Phys. Rev. B **43**, 130 (1991).

[49] L. R. Walker and R. E. Walstedt, Phys. Rev. B **22**, 3816 (1980).

[50] Y.-H. Li, Phys. Rev. Lett. **69**, 1819 (1992); G. S. Jeon, S. Kim, and M. Y. Choi, Phys. Rev. B **51**, 16211 (1995).

[51] M. Y. Choi and S. Y. Park, Phys. Rev. B **60**, 4070 (1999).